JOURNAL OF Applied Polymer SCIENCE

Reactive, Intumescent, Halogen-Free Flame Retardant for Polypropylene

Guixun Li, Wanjie Wang, Shaokui Cao, Yanxia Cao, Jingwu Wang
School of Materials Science and Engineering, Zhengzhou University, Zhengzhou 450052, China
Correspondence to: J. Wang (E-mail: jingwuwang@zzu.edu.cn)

ABSTRACT: A reactive, intumescent, halogen-free flame retardant, 2-({9-[(4,6-diamino-1,3,5-triazin-2-yl)amino]-3,9-dioxido-2,4,8,10-tetraoxa-3,9-diphosphaspiro[5.5]undecan-3-yl}oxy)ethyl methacrylate (EADP), was synthesized through a simple three-step reaction from phosphorus oxychloride, pentaerythritol, hydroxyethyl methacrylate, and melamine. EADP exhibited excellent thermal stability and char-forming ability, as revealed by thermogravimetric analysis (TGA) and scanning electron microscopy (SEM). The TGA results show that the temperature at 5% weight loss was 297.8°C and the char yield at 700°C was 51.75%. SEM observation revealed that the char showed a continuous and compact surface and a cellular inner structure with different sizes. Composite of polypropylene (PP) with a 25 wt % addition of EADP (PP/EADP25) passed the UL-94 V-0 rating and showed a limiting oxygen index value of 31.5. Compared with those of neat PP, the flexural strength and modulus values of PP/EADP25 were somewhat improved, the tensile strength was basically unchanged, and the notched Izod impact strength was slightly decreased. © 2013 Wiley Periodicals, Inc. J. Appl. Polym. Sci. **2014**, *131*, 40054.

KEYWORDS: flame retardance; mechanical properties; polyolefins; thermal properties

Received 16 March 2013; accepted 11 October 2013
DOI: 10.1002/app.40054

INTRODUCTION

Halogen-containing flame retardants for polyolefin flame retardation have been more and more restricted in recent years because of environmental concerns, and halogen-free flame retardants are highly desired.[1] Intumescent flame retardants (IFRs) have provided an effective method because of their low toxicity and low smoke production during burning. IFRs, which combine an acid source, a blowing agent, and a char-forming agent within one molecule, have received more and more attention.[2–4] A halogen-free IFR, pentaerythritol spirobisphosphoryl dicyandiamide (SPDC), which has a ratio of phosphorus, nitrogen, and carbon of 1.00:1.81:2.13, was reported to have a char yield of 39.2 wt % at 600°C in nitrogen.[5] Polypropylene (PP) with 30 wt % SPDC addition passed the UL-94 V-0 rating and showed a limiting oxygen index (LOI) value of 32.5, and the tensile strength, flexural strength, and notched Izod impact strength decreased only by 4.0, 8.1, and 11.4%, respectively, as compared with those of neat PP. A modified composition with a ratio of phosphorus to nitrogen to carbon of 1.00:1.67:1.59 adjusted with ammonium polyphosphate showed an even better flame-retardation behavior for PP.[6] An oligomeric phosphorous- and nitrogen-containing IFR, poly(4,4-diamino diphenyl methane-*o*-bicyclic pentaerythritol phosphate), which had a phosphorus to nitrogen to carbon ratio of 1.00:0.45:3.48, was reported to have a char yield of 50.6% at 600°C under nitrogen.[7,8] PP with a 30 wt % poly(4,4-diamino diphenyl methane-*o*-bicyclic pentaerythritol phosphate) addition showed a LOI value of 28.0, whereas the tensile strength was reduced to 71.43% that of neat PP. Thus, it could be considered that a good flame-retardation effect for an IFR is determined by a proper ratio of the acid source to the blowing agent to the char-forming agent.

In this article, we report a novel, reactive intumescent halogen-free flame retardant, 2-({9-[(4,6-diamino-1,3,5-triazin-2-yl)amino]-3,9-dioxido-2,4,8,10-tetraoxa-3,9-diphosphaspiro[5.5]undecan-3-yl}oxy)ethyl methacrylate (EADP), synthesized through a simple three-step reaction from phosphorus oxychloride ($POCl_3$), pentaerythritol, hydroxyethyl methacrylate (HEMA), and melamine. Spirocyclic pentaerythritol bisphosphorate disphosphoryl chloride (SPDPC) was first synthesized through the reaction of pentaerythritol with phosphorus oxychloride, which could act as the acid source and the char-forming agent. Subsequently, SPDPC was reacted with HEMA and melamine in turn to allow EADP to have a reactive group and a blowing agent. The obtained EADP was characterized by Fourier transform infrared (FTIR) spectroscopy, ^{1}H-NMR, and elemental analysis. Composites of PP with EADP (PP/EADP) were prepared through reactive blending, and the mechanical properties and

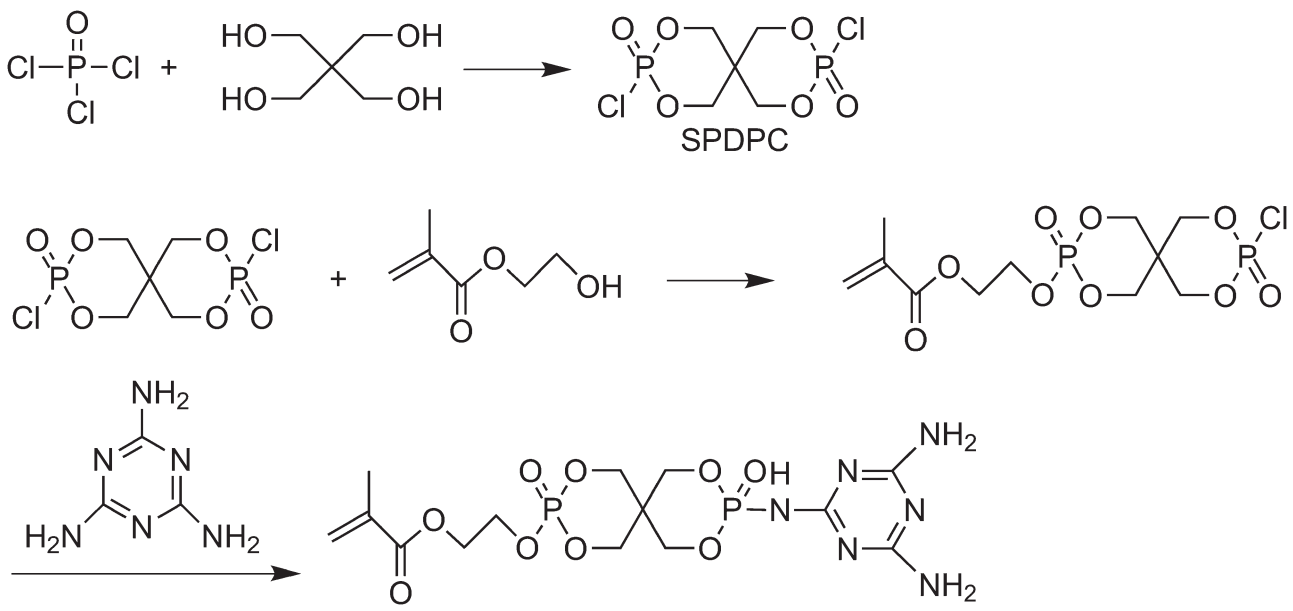

Scheme 1. Synthetic process for EADP.

flame-retardation behavior were evaluated in comparison with those of neat PP.

EXPERIMENTAL

Materials

Analytically pure phosphorus oxychloride was provided by Tianjin Fuyu Fine Chemical Co., Ltd. Pentaerythritol, HEMA, melamine, acetonitrile, and triethylamine, all with analytical purity, were obtained from Tianjin Kermel Chemical Reagent Co., Ltd. SPDPC was synthesized from phosphorus oxychloride and pentaerythritol.[9] PP (F401) was obtained commercially from Luoyang Petrochemical Co., Ltd. Ethylene-propylene-diene monomer (EPDM, 3745P) and styrene-butadiene-styrene copolymer (SBS, 796) were obtained commercially from Baling Petrochemical Co., Ltd., and DuPont, respectively. A commercial IFR, provided by Puyang Chengke Chemical Technology Co., was used for comparative study.

Synthesis of EADP

SPDPC (29.70 g, 0.1 mol) and 400 mL of acetonitrile were placed in a 1000-mL flask equipped with a thermometer, a magnetic stirrer, a condenser, and a feeding funnel, into which 13.01 g (0.1 mol) of HEMA was added dropwise within 4 h under stirring at 25 ± 1°C. Then, 10.12 g (0.1 mol) triethylamine was added and kept stirred for 12 h to remove the hydrochloric acid produced. Subsequently, 12.60 g (0.1 mol) of melamine and 10.12 g (0.1 mol) of triethylamine were added, and the mixture was heated to 60 ± 1°C and kept there for 12 h. The reaction mixture was cooled slowly to room temperature and filtered. The white solid was washed with water and vacuum-dried at 60°C to a constant weight. The product was obtained at 73.20% yield, and the reaction process is illustrated in Scheme 1.

Preparation of the PP/EADP Composites

The PP/EADP composites were prepared with reactive blending in a high-speed mixer and then extruded with a twin-screw extruder (SHJ-20, Nanjing Giant Machinery Co., Ltd.) at a temperature profile of 175, 185, 195, 205, and 195°C. The composites were prepared from PP, EADP, and an elastomer (with an EPDM/SBS ratio of 4:1 in weight) with compositions of 70/20/10, 65/25/10, 60/30/10, and 55/35/10 for the PP/EADP20, PP/EADP25, PP/EADP30, and PP/EADP35 samples, respectively. The PP/EADP composite pellets dried at 105°C for 4 h were injection-molded at 170–210°C into test samples for measurements in an injection-molding machine (HTF80W2, Ningbo Haitian Co., Ltd.).

Characterization

FTIR measurements were performed on a Nicolet Avatar360 FTIR spectrophotometer in the range 4000–400 cm^{-1} with KBr pellets for EADP and hot-pressed films for the PP/EADP composites. The carbon and nitrogen contents in EADP were investigated by a Flash EA 1112 elemental analyzer, and the phosphorus content was measured by a gravimetric quimociac technique.[10] ^{1}H-NMR spectra were recorded on a Bruker DPX-400 spectrometer with deuterated dimethyl sulfoxide as the solvent and tetramethylsilane as the internal reference.

For the determination of the apparent conversion of EADP, the PP/EADP composite and xylene were added to a three-necked flask, heated to reflux to dissolve the sample, and then poured slowly into a beaker with 36% acetic acid to extract the unreacted and homopolymerized EADP. The residue after filtration was repeatedly dissolved in xylene and washed with 36% acetic acid until a constant weight was reached. The unreacted and homopolymerized EADP extracts were dried and weighed. The apparent conversion of EADP, which could be regarded as the EADP grafted onto the polymer matrix, was calculated by the following equation:

$$T\% = \frac{m \times w\% - m_1}{m \times w\%} \times 100\%$$

where $T\%$ is the apparent conversion of EADP, $w\%$ is the content of EADP in the PP/EADP composite, m is the weight of the PP/EADP composite, and m_1 is the weight of the extracts.

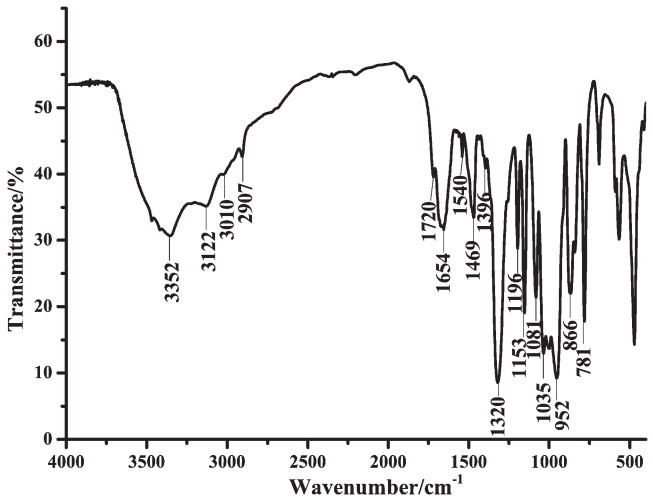

Figure 1. FTIR spectrum of EADP.

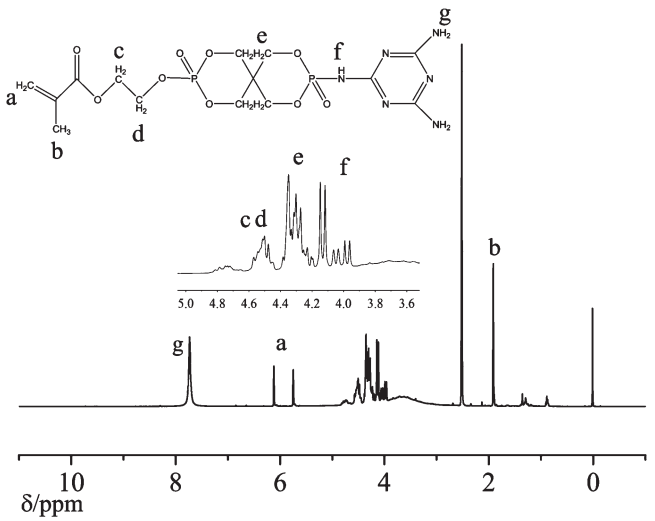

Figure 2. ^{1}H-NMR spectrum of EADP.

Thermogravimetric analysis (TGA) was performed on a Netzsch STA 449 C analyzer at a heating rate of 10°C/min. A 4–5-mg sample was examined in a nitrogen atmosphere from ambient temperature to 700°C.

Morphological observations were carried out with an S-4700 scanning electron microscope (Hitachi, Japan). The EADP samples were calcined in a muffle furnace at 600°C for 10 min, and the residual chars were collected for the observation.

The tensile strength and flexural strength were measured with a CMT6104 machine (Shenzhen SANS Test Equipment Co., Ltd.) according to GB/T 1040-2006 and GB/T 9341-2008 standards. The notched Izod impact strength was obtained with an XJU-2 Izod impact instrument (Hebei Chengde Precision Equipment Co.) according to GB/T 1843-2008 standards. The flammability of the PP/EADP composites were evaluated by LOI and UL94 tests. The LOI values were measured with an HC-2C oxygen index meter (Jiangning, China) according to ASTM D 2863-09 at room temperature. The UL-94 tests were performed according to an ASTM D 3801 testing procedure on a CZF-2 instrument (Jiangning, China) with samples of 125 × 12.7 × 3.2 mm^3.

RESULTS AND DISCUSSION

Characterization of EADP

The FTIR spectrum of EADP is shown in Figure 1. The absorption of the carbonyl group was observed at 1720 cm^{-1}, and the peak at 1654 cm^{-1} was associated with the stretching mode of C═C; this indicated that HEMA was successfully introduced into the target product.[2,11,12] The absorptions at 3352 and 3122 cm^{-1} corresponded to the stretching vibrations of N—H,[13,14] and those at 1540 and 1396 cm^{-1} were the signals for the vibrations of the triazine ring.[15] The absorption at 781 cm^{-1} was assigned to the P—N stretching band;[16] this indicated that melamine was also introduced into the target product of EADP. The peak at 1320 cm^{-1} was associated with the stretching mode of P═O, and the peak at 1035 cm^{-1} was assigned to P—O—C in the phosphate.[17] This indicated the existence of bicyclic phosphate in EADP.[18]

Figure 2 shows the ^{1}H-NMR spectrum of EADP. The signal at $\delta = 1.90$ corresponded to the protons of the methyl group;[19] the signals between $\delta = 3.94$ and 4.14 belonged to the protons of amino group adjacent to the phosphate. The multiple peaks between $\delta = 4.22$ and 4.37 corresponded to the methylene protons of the bicyclic phosphate,[20] and the complicated signals at about $\delta = 4.40$–4.62 were assigned to the ethylene protons of the methacrylate. The two doublets at $\delta = 5.73$ and 6.10 originated from the protons of the double bond,[19] whereas the singlet at $\delta = 7.72$ was attributed to the amino protons of melamine. The broad dispersive base between $\delta = 3.00$ and 4.20 might have been derived from a polymeric or oligomeric side product associated with SPDPC formation from the reaction of phosphorus oxychloride with pentaerythritol. The poor inosculation between the calculated and observed values in the elemental analysis of EADP, which is shown in Table I, also suggested the formation of a polymeric or oligomeric side product. However, for flame-retardation purposes and from an economical perspective, we believe that the prepared EADP was not necessarily completely pure. From the results of the elemental analysis shown in Table I, the observed values for phosphorus, carbon, and nitrogen were basically consistent with the calculated values for EADP.

Thermal Stability and Char-Forming Ability of EADP

The TGA and differential thermogravimetry (DTG) curves of EADP in a nitrogen atmosphere are presented in Figure 3. The temperature at 5% weight loss ($T_{5\%}$) was measured as 297.8°C; this would guarantee enough thermal stability under the molding process of PP, polyethylene, and so on. A higher char yield may benefit flame retardation,[21] and the char yield of EADP

Table I. Elemental analysis for EADP

	C (%)	P (%)	N (%)	H (%)
Calculated value	35.01	12.90	17.50	4.62
Observed value	34.12	12.02	20.25	4.74

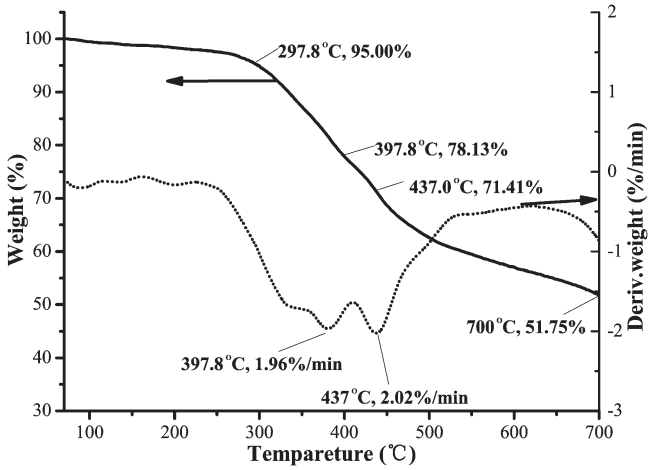

Figure 3. TGA and DTG curves of EADP.

was measured as 51.75% at 700°C; this indicated an excellent char-forming ability.[22] The first stage for rapid weight loss of EADP was at 397.8°C, the corresponding mass loss rate was 1.96%/min, and the fraction of the residue remaining was 78.13%. The weight loss of the first stage was due to the decomposition of P—O—C to form crosslinked poly(phosphoric acid)s and release gases such as NH_3 and H_2O.[23] The second stage of rapid weight loss was at 437°C and the fraction of residue remaining was 71.41%. The second stage was responsible for the residual char formatting.[24]

Figure 4 shows digital photographs of EADP before and after calcination. Intact char was formed after EADP calcination, and the volume of residue char increased significantly. The scanning electron microscopy (SEM) micrographs (Figures 5 and 6) revealed that the char had a continuous and compact surface and a cellular inner structure with different sizes. This indicated that the flame retardant released NH_3 and water vapor to make the molten carbon residue intumescent during the thermal decomposition process. A continuous and intact char layer could not only prevent the oxygen and heat from reaching the underlying substrate but also block the production of small molecules by thermal degradation; this demonstrated the effective work of a flame retardant.[25]

To examine the structural and compositional changes of EADP during thermal degradation, FTIR spectra were measured with samples taken at different temperatures, as shown in Figure 7. The main characteristic absorption peaks of EADP were at 3352 and 3122 cm^{-1} (N—H), 1720 cm^{-1} (C═O), 1654 cm^{-1} (C═C), 1320 cm^{-1} (P═O), and 1035 cm^{-1} (P—O—P) at 25°C. For the sample taken at 290°C, the characteristic absorption peak at 3300 cm^{-1} became weak and broad; this suggested the elimination of NH_3 from melamine and the dehydration from the EADP;[26] meanwhile, the characteristic absorption peak at 1720 cm^{-1} disappeared, and the peaks at 1299 and 1024 cm^{-1} also became weak. For the sample taken at 350°C, there appeared a new peak at 1633 cm^{-1}; this indicated the formation of an aromatic structure.[24,27] Furthermore, for the sample taken at 550°C, all of the peaks except that of P—O—P became weak. On the basis of the previous analysis, EADP first formed phosphoric acid when heated. This reacted with the carbon source and dehydrated, and the gas source released noncombustible gases to promote the formation of an intumescent char layer.

Flame Retardation and Thermal Stability of the PP/EADP Composites

To evaluate the flame-retardation behaviors of the PP/EADP composites, we conducted LOI and UL-94 tests, and the results are listed in Table II, together with those of the neat PP for comparison. The LOI value of PP was 18.2, which indicated that it was highly flammable. However, the flame retardation of PP/EADP was obviously enhanced in comparison with that of PP. PP/EADP25, that is, the composite containing 25 wt % of EADP, passed the UL-94 V-0 rating and had an LOI value of 31.5. We also found that the LOI value of the PP/EADP composites basically increased with increasing EADP content. These results of the flame-retardation effect were in good agreement with those of the reference literature.[5]

TGA and DTG curves of the PP/EADP composites are shown in Figures 8 and 9. It was clear that PP exhibited only a one-step degradation process with a maximum mass loss rate at about 343°C without any residual char left at about 600°C.

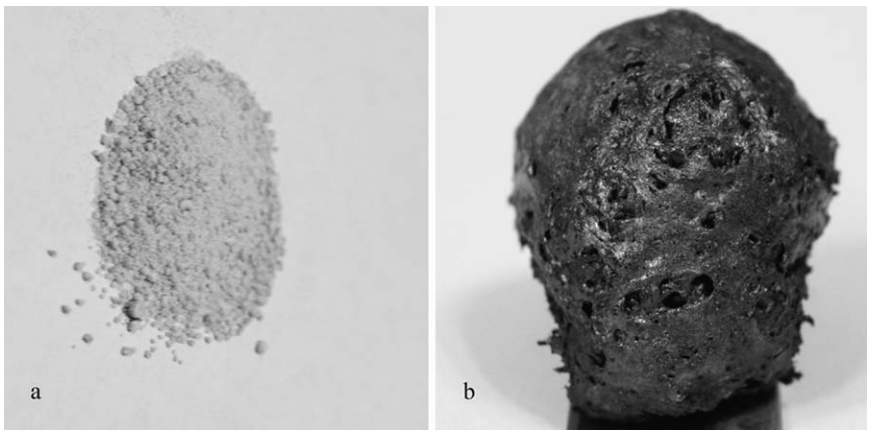

Figure 4. Digital photos of EADP (a) before and (b) after calcination.

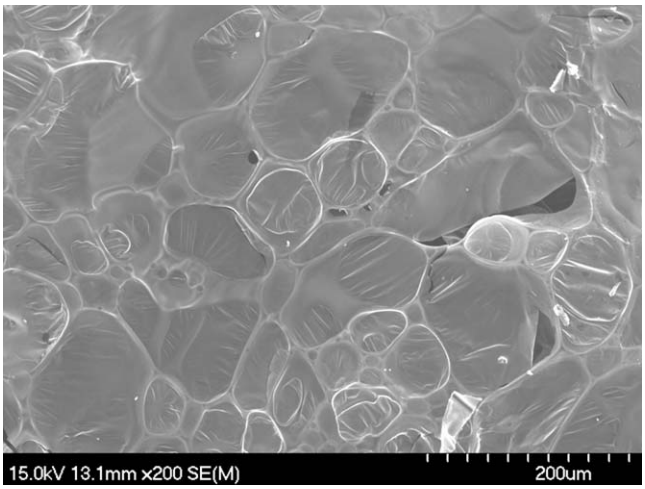

Figure 5. SEM image of the char surface of EADP.

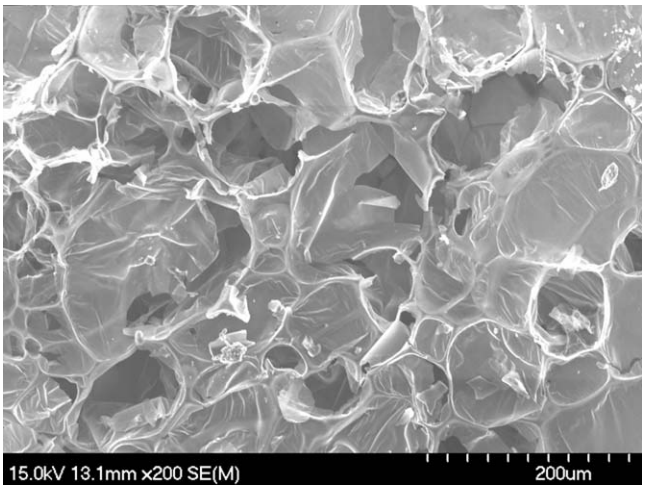

Figure 6. SEM image of the char inner structure of EADP.

The PP/EADP composites showed a major weight loss stage (at about 250–350°C) and a minor weight loss stage (at about 460–650°C). We also found that with increasing EADP content, the PP/EADP composite started to decompose at a higher temperature with a lower maximum degradation rate (R_{max}) and higher char yield. Table II gives the thermal analysis data obtained from TGA; it was clear that the PP/EADP composite showed a higher $T_{5\%}$ and a lower maximum decomposition rate. This also indicated that the addition of EADP imparted the PP/EADP composite with a higher char yield and improved the stability of the residual char at higher temperatures.[28]

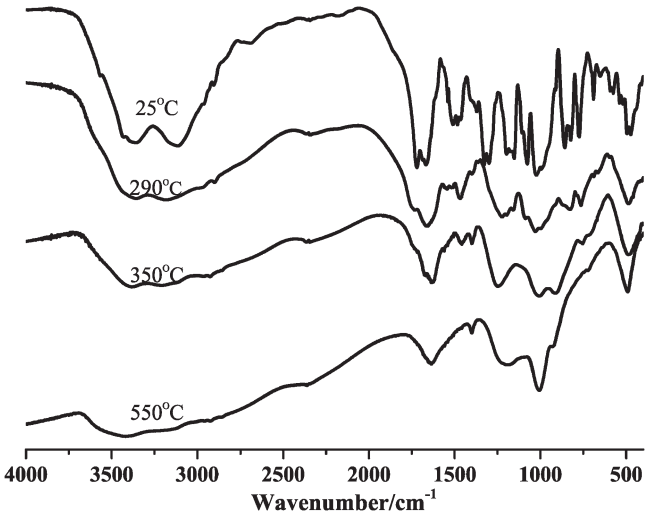

Figure 7. FTIR spectra of EADP at different pyrolysis temperatures.

Figure 10 displays the SEM micrograph of the intumescent char obtained from PP/EADP30. It was obvious that the intumescent char from PP/EADP30 was very compact and may have acted as an insulating barrier to prevent the heat transfer between the flame zone and the underlying substrate and to protect the substrate from heat and fire.[29]

Dispersion of EADP in the PP/EADP Composites

To make clear the dispersion statues of the EADP in PP/EADP, that is, whether a solely physical mixing or chemical reactions between the EADP and PP matrix happened in the compounding process, extraction experiments and corresponding FTIR characterization were conducted for the PP/EADP composites, which could provide important information if the reactive IFR was really chemically reactive and could also provide evidence for understanding the composite morphology. Figure 11 shows the FTIR spectra of the EADP and extracts of PP/EADP30 with aqueous acetic acid. The absorption at 1656 cm^{-1}, which was assignable to the stretching mode of the C=C band,[30] appeared in both the FTIR spectra of EADP and the extracts of PP/EADP30; this indicated that the extracts contained unreacted EADP. The characteristic absorptions of PP,[31,32] such as those at 998, 973, and 841 cm^{-1}, were not observed in the FTIR spectra

Table II. Thermal Analysis Data and Flame-Retardation Behavior of the PP/EADP Composites

Sample	$T_{5\%}$ (°C)	R_{max} (%/min)	T_{max} (°C)	Char yield (%)	LOI (%)	UL-94
PP	256	14.53	343	—	18.2	No rating
PP/EADP20	267	6.31	383	6.24	29.5	V-1
PP/EADP25	285	6.05	385	10.45	31.5	V-0
PP/EADP30	287	5.73	370	19.61	32.2	V-0
PP/EADP35	317	5.56	388	24.75	33.0	V-0

T_{max}, maximum degradation temperature. The char yield was measured at 600°C.

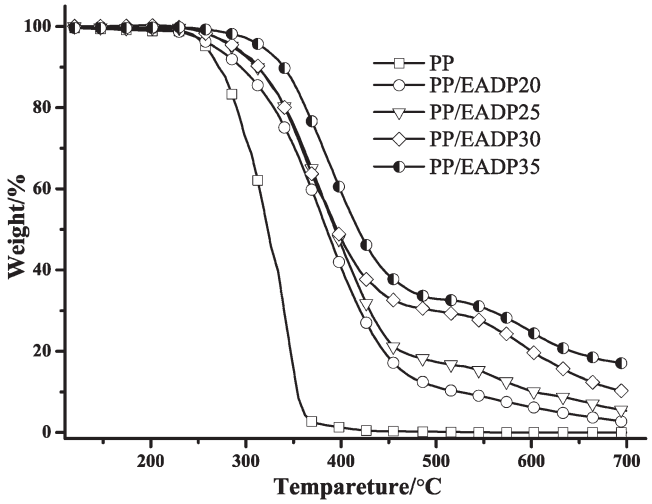

Figure 8. TGA curves of the PP/EADP composites.

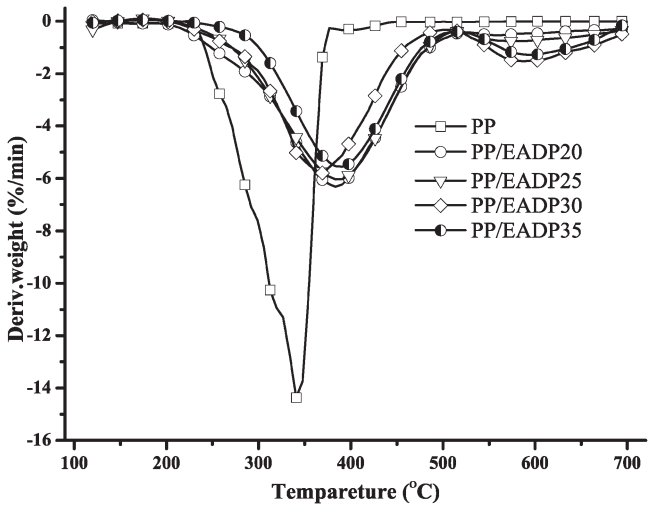

Figure 9. DTG curves of the PP/EADP composites.

of the extracts, as shown in Figure 12. This proved that the extracts with aqueous acetic acid did not contain PP and the graft copolymer of EADP and PP.

For the monomer of methacrylic acid esters, its characteristic absorption around 1453 cm^{-1} split into two absorptions when homopolymerized.[33,34] Such a characteristic absorption was observed at 1468 cm^{-1} for EADP. In the compounding process for making PP/EADP composites, when homopolymerization happens, the splitting of the 1468 cm^{-1} signal is observed, and an absorption for quaternary carbon atom around 1245 cm^{-1} also appears.[35] All of these signals were found in the FTIR spectra of the extracts with aqueous acetic acid, as shown in Figure 13(B); this indicated that the EADP homopolymer was contained in the extracts with aqueous acetic acid.

The FTIR spectrum of the PP/EADP30 residue after extraction is shown in Figure 13(C), from which the typical absorption at 1654 cm^{-1} for the C═C double bond was not observed; this illustrated the complete remove of unreacted EADP after extraction. Similarly, the splitting of the 1468-cm^{-1} signal and the absorption for the quaternary carbon atom around 1245 cm^{-1} were also not observed; this suggested that the EADP homopolymer was extracted completely. The constant-weight experiments for the extracts of PP/EADP30, shown in Figure 14, provided more evidence for the complete extraction of the unreacted and homopolymerized EADP. The FTIR spectrum of the PP/EADP30 extraction residue showed the characteristic peaks of EADP at 3348 cm^{-1} (N—H), 1716 cm^{-1} (C═O), and 1020 cm^{-1} (P—O—C) and those of PP at 2952, 2868, 998, 973, and 841 cm^{-1}; this indicated the existence of the graft copolymer of EADP and PP.

The polarized optical microscopy (POM) images of the PP/EADP30 and PP/IFR30 composites are shown in Figures 15 and 16, respectively. We used PP/IFR30 as a sample for comparison by compounding 30 wt % of the flame retardant IFR, a commercial IFR, with PP. Large and unevenly dispersed particles were observed in the PP/IFR30 composite; this

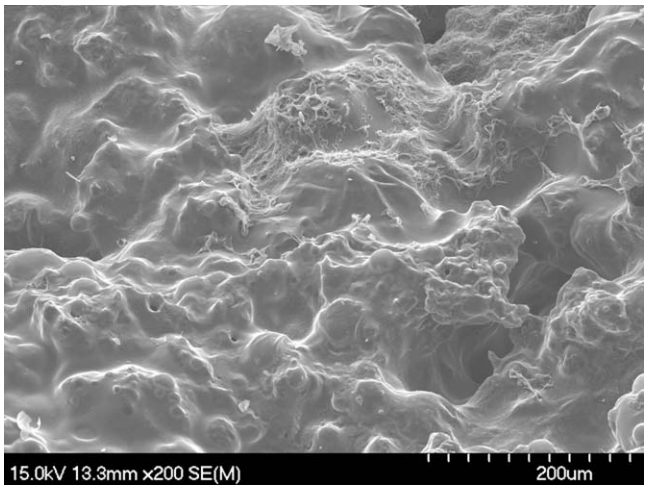

Figure 10. SEM micrograph of the residual char from PP/EADP30.

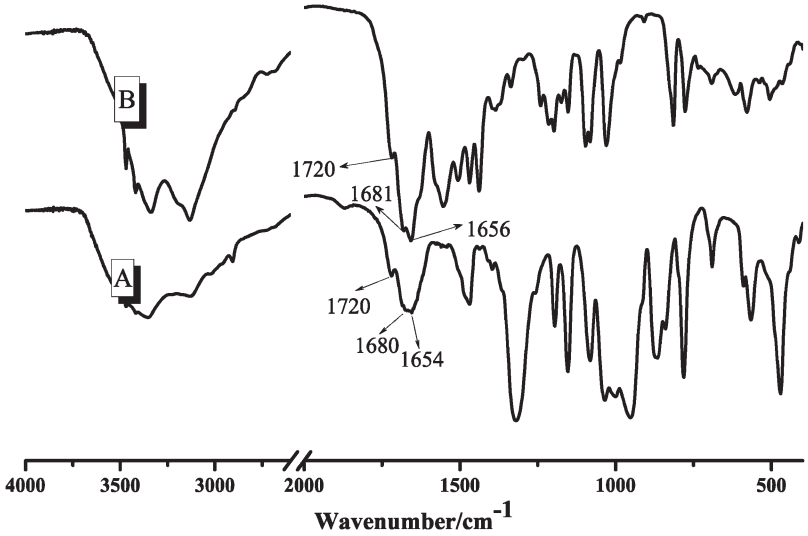

Figure 11. FTIR spectra of the (A) EADP and (B) extracts with aqueous acetic acid.

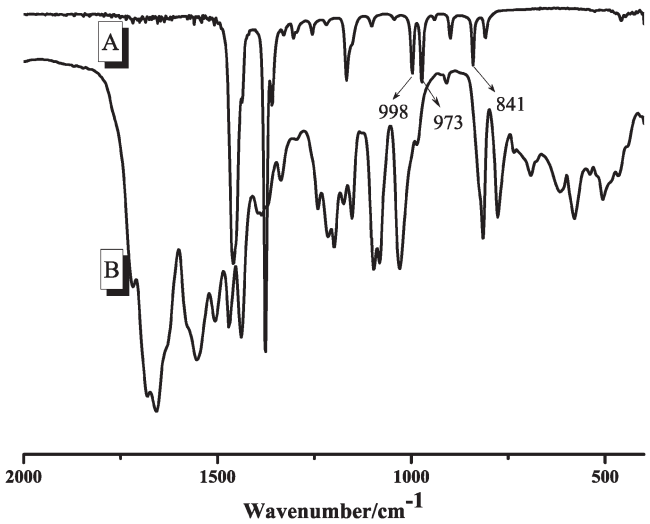

Figure 12. FTIR spectra of the (A) PP and (B) extracts with aqueous acetic acid.

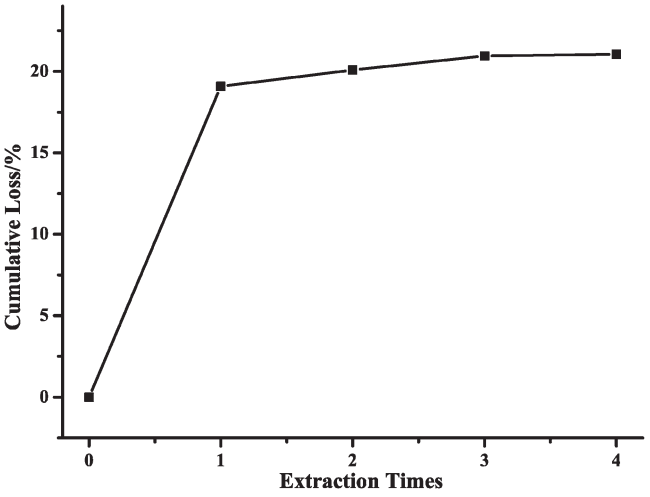

Figure 14. Constant weight curve of the PP/EADP30 extracts by aqueous acetic acid.

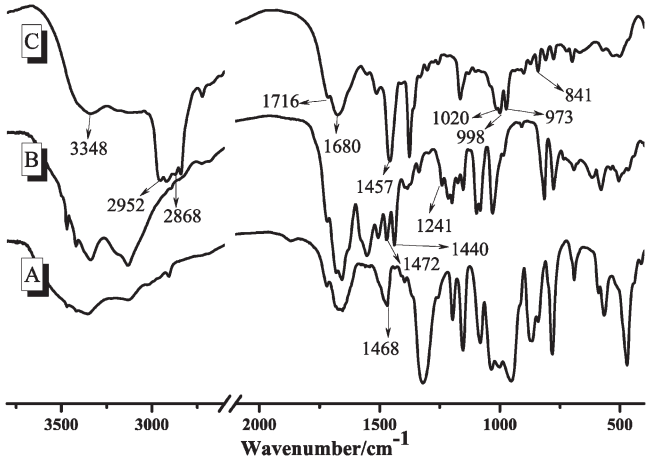

Figure 13. FTIR spectra of the (A) EADP, (B) extracts with aqueous acetic acid, and (C) PP/EADP30 residue after extraction.

Figure 15. POM image of the ultrathin section from PP/EADP30 (200×).

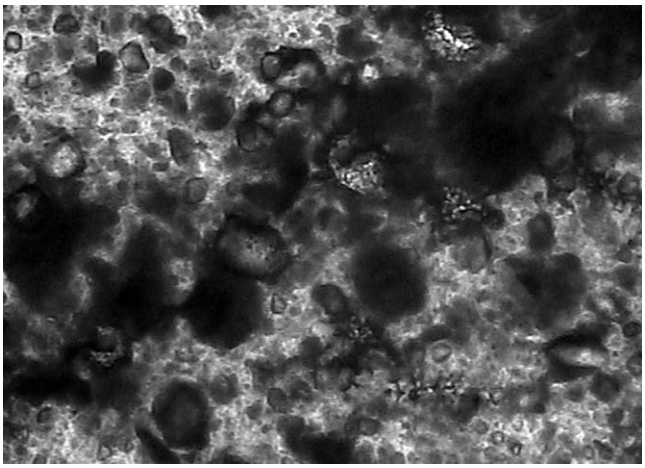

Figure 16. POM image of the ultrathin section from PP/IFR30 (200×).

strongly suggested an immiscible dispersion. The size of the dispersed particles in the PP/EADP30 composite was much smaller, and the particle size distribution was more uniform; this may have been derived from the compatibilization enhancement contributed by the copolymer of EADP grafted on PP. The apparent conversion of EADP obtained from the extraction experiment was calculated as 29.83%; this was regarded as the percentage of EADP that was reacted with PP.

Mechanical Properties of the PP/EADP Composites

The mechanical properties of the PP/EADP composites are listed in Table III. Compared with those of neat PP, the flexural strength and modulus values of the PP/EADP composites increased with increasing EADP content. The flexural strength and modulus of PP/EADP25 were increased by 8.37 and 23.36%, respectively, as those of neat PP. In the PP/EADP composite, EADP could be regarded as a rigid phase, and the flexural properties of the composite should have had an increase according to the mixing rules.[36] On the other hand, the tensile strength and notched Izod impact strength of the composite showed a slightly decrease with the increase in the EADP content; this may have been due to the formation of some EADP aggregates during compounding. In summary, the PP/EADP composites showed a good flame-retardation behavior without an appreciable loss in the mechanical properties.

Table III. Mechanical Properties of the PP/EADP Composites

Sample	Tensile strength (MPa)	Flexural modulus (GPa)	Flexural strength (MPa)	Impact strength (kJ/m^2)
PP	26.57	1.07	26.52	5.59
PP/EADP20	27.78	1.24	27.40	5.42
PP/EADP25	27.18	1.32	28.74	5.30
PP/EADP30	26.58	1.41	28.94	5.27
PP/EADP35	25.46	1.52	30.01	5.02

CONCLUSIONS

A novel IFR (EADP) was synthesized; it was composed of an acid source, a blowing agent, and a char-forming agent in one molecule with a suitable ratio of phosphorus, nitrogen, and carbon. EADP had a good thermal stability, and TGA measurement showed that $T_{5\%}$ was 297.8°C with a char yield of 51.75% at 700°C. The volume of the residue char increased significantly after calcination, and the char showed a continuous and compact surface and a cellular inner structure with different sizes, as revealed by SEM observation. The PP/EADP composites showed a gradually increased LOI value with increasing EADP content. With a 25 wt % addition of EADP, the PP/EADP25 composite showed a LOI value of 31.5 and passed the UL-94 V-0 rating. Because a reactive group existed in the EADP molecule, its compatibility with polyolefin was greatly enhanced, and this resulted in good retention of the mechanical properties of the composite. The tensile strength basically remained unchanged, the notched Izod impact strength showed a slight decrease, and the flexural strength and modulus increased by 8.37 and 23.36%, respectively. This suggested that EADP is an effective IFR with limited effects on the mechanical properties of PP.

REFERENCES

1. Dai, J. F.; Li, B. *J. Appl. Polym. Sci.* **2010**, *116*, 2157.
2. Yan, L.; Zheng, Y. B.; Liang, X. B.; Ma, Q. *J. Appl. Polym. Sci.* **2010**, *115*, 1032.
3. Huang, J. Q.; Zhang, Y. Q.; Yang, Q.; Liao, X.; Li, G. X. *J. Appl. Polym. Sci.* **2012**, *123*, 1636.
4. Feng, C.; Zhang, Y.; Liu, S. W.; Chi, Z. G.; Xu, J. R. *J. Appl. Polym. Sci.* **2012**, *123*, 3208.
5. Xiang, H. W.; Sun, C. Y.; Jiang, D. W.; Zhang, Q. B.; Dong, C. M.; Liu, L. *J. Vinyl. Addit. Technol.* **2010**, *16*, 261.
6. Xiang, H. W.; Sun, C. Y.; Jiang, D. W.; Zhang, Q. B.; Dong, C. M.; Liu, L. *J. Vinyl. Addit. Technol.* **2010**, *16*, 161.
7. Song, P. A.; Fang, Z. P.; Tong, L. F.; Xu, Z. B. *Polym. Eng. Sci.* **2009**, *49*, 1326.
8. Song, P. A.; Shen, Y.; Du, B. X.; Peng, M.; Shen, L.; Fang, Z. P. *ACS Appl. Mater. Interfaces* **2009**, *1*, 452.
9. Rätz, R.; Sweeting, O. J. *J. Org. Chem.* **1963**, *28*, 1608.
10. Shaver, L. A. *J. Chem. Educ.* **2008**, *85*, 1097.
11. Wang, G. A.; Wang, C. C.; Chen, C. Y. *Polym. Degrad. Stab.* **2006**, *91*, 2683.
12. Xing, W. Y.; Song, L.; Lv, P.; Jie, G. X.; Wang, X.; Lv, X. Q.; Hu, Y. A. *Mater. Chem. Phys.* **2010**, *123*, 481.
13. Hu, X. P.; Li, W. Y.; Wang, Y. Z. *J. Appl. Polym. Sci.* **2004**, *94*, 1556.
14. Chen, L. J.; Tai, Q. L.; Song, L.; Xing, W. Y.; Jie, G. X.; Hu, Y. *Express Polym. Lett.* **2010**, *4*, 539.
15. Zhang, Y. J.; Lu, Y. B.; Guo, F.; Peng, C.; Li, M. M.; Xu, W. *J. Polym. Adv. Technol.* **2012**, *23*, 166.
16. Yu, Y. M.; Fu, S. Y.; Song, P. A.; Luo, X. P.; Jin, Y. M.; Lu, F. Z.; Wu, Q.; Ye, J. W. *Polym. Degrad. Stab.* **2012**, *97*, 541.

17. Mouritz, A. P.; Gibson, A. G. Fire Properties of Polymer Composite Materials; Springer: Waterloo, Canada, **2006**.
18. Chen, G. H.; Yang, B.; Wang, Y. Z. *J. Appl. Polym. Sci.* **2006**, *102*, 4978.
19. Guan, J. P.; Chen, G. Q. *Fire Mater.* **2010**, *34*, 261.
20. Zhi, Y. J.; Yong, Y.; Ru, Y. Z.; Xin, C. L.; Yu, F. Z. *Chin. Chem. Lett.* **2008**, *19*, 277.
21. Vijayakumar, C.; Mathan, N.; Sarasvathy, V.; Rajkumar, T.; Thamaraichelvan, A.; Ponraju, D. *J. Therm. Anal. Calorim.* **2010**, *101*, 281.
22. Song, P. A.; Tong, L. F.; Fang, Z. P. *J. Appl. Polym. Sci.* **2008**, *110*, 616.
23. Çanak, T. Ç.; Serhatlı, İ. E. *Prog. Org. Coat.* **2013**, *76*, 388.
24. Bugajny, M.; Bourbigot, S.; Le Bras, M.; Delobel, R. *Polym. Int.* **1999**, *48*, 264.
25. Li, L.; Wei, P.; Li, J.; Jow, J.; Su, K. *J. Fire Sci.* **2010**, *28*, 523.
26. Peng, H. Q.; Zhou, Q.; Wang, D. Y.; Chen, L.; Wang, Y. Z. *J. Ind. Eng. Chem.* **2008**, *14*, 589.
27. Cai, Y. B.; Hu, Y.; Song, L.; Xuan, S. Y.; Zhang, Y.; Chen, Z. Y.; Fan, W. C. *Polym. Degrad. Stab.* **2007**, *92*, 490.
28. Chen, D. Q.; Wang, Y. Z.; Hu, X. P.; Wang, D. Y.; Qu, M. H.; Yang, B. *Polym. Degrad. Stab.* **2005**, *88*, 349.
29. Wang, D. Y.; Liu, Y.; Ge, X. G.; Wang, Y. Z.; Stec, A.; Biswas, B.; Hull, T. R.; Price, D. *Polym. Degrad. Stab.* **2008**, *93*, 1024.
30. Yu, B.; Zeng, G.; Liu, Y. *Acta Phys. Sin-Ch. Ed.* **1966**, *22*, 62.
31. Yang, Z.; Qian, R. *Polym. Commun.* **1965**, 69.
32. Zhang, M.; Polymer Research Methods; China Light Industry: Beijing, **2000**.
33. Ma, Y.; Zheng, X.; Si, F.; Li, Y. *J. Qingdao Univ. Nat. Sci. Ed.* **2004**, *12*.
34. Trujillo, N. J.; Baxamusa, S. H.; Gleason, K. K. *Chem. Mater.* **2009**, *21*, 742.
35. Wong, S. F. Fourier Transform Infrared Spectroscopy Analysis; Chemical Industry: Beijing, **2010**.
36. Wang, J. W. Plastic Modification Technology; Chemical Industry: Beijing, **2004**.